Analyst

PAPER

View Article Online
View Journal | View Issue

Cite this: *Analyst*, 2014, **139**, 4620

Lab-on-a-drop: biocompatible fluorescent nanoprobes of gold nanoclusters for label-free evaluation of phosphorylation-induced inhibition of acetylcholinesterase activity towards the ultrasensitive detection of pesticide residues

Ning Zhang,[a] Yanmei Si,[a] Zongzhao Sun,[a] Shuai Li,[a] Shuying Li,[a] Yuehe Lin[b] and Hua Wang*[a]

A simple, sensitive, selective, and "lab-on-a-drop"-based fluorimetric protocol has been proposed using biocompatible fluorescent nanoprobes of gold nanoclusters (AuNCs) for the label-free evaluation of the catalytic activity and phosphorylation of acetylcholinesterase (AChE) under physiologically simulated environments. Protein-stabilized AuNCs were prepared and mixed with acetylthiocholine (ATC) serving as "a drop" of fluorimetric reaction substrate. The AChE-catalyzed hydrolysis of ATC releases thiocholine to cause the aggregation of the AuNCs towards a dramatic decrease in fluorescence intensities, which could be curbed by the phosphorylation-induced inhibition of AChE activity when exposed to organophosphorus compounds (OPs). The reaction procedures and conditions of AChE catalysis and phosphorylation were monitored by fluorimetric measurements and electron microscopy imaging. Moreover, a selective and ultrasensitive fluorimetric assay has been tailored for the detection of pesticide residues using dimethyl-dichloro-vinyl phosphate (DDVP) as an example. Investigation results indicate that the specific catalysis and irreversible OP-induced phosphorylation of AChE, in combination with sensitive fluorimetric outputs could facilitate the detection of total free OPs with high selectivity and sensitivity. A linear concentration of DDVP ranging from 0.032 nM to 20 nM could be obtained with a detection limit of 13.67 pM. Particularly, pesticide residues of DDVP in vegetable samples were quantified down to ~36 pM. Such a label-free "lab-on-a drop"-based fluorimetry may promise wide applications for the evaluation of the physiological catalytic activity of various enzymes (*i.e.*, cholinesterase), and especially for monitoring the direct phosphorylation biomarkers of free OPs towards rapid and early warning, and accurate diagnosis of OP exposure.

Received 12th May 2014
Accepted 27th June 2014

DOI: 10.1039/c4an00855c

www.rsc.org/analyst

1. Introduction

Highly toxic organophosphorus compounds (OPs), including nerve agents and organophosphate pesticides, are severely threatening public safety and the environment. Nerve agents as toxic chemical warfare agents[1] are commonly misused in modern war and terrorist attacks, such as the Tokyo subway attack in 1995 and the events in Syria in 2013. In particular, pesticides are used worldwide in agriculture leading to their widespread contamination in air, water, soil and agricultural products.[2] As a way of invading and attacking the human body, OPs may bind to cholinesterase like acetycholinesterase (AChE) at certain active sites of amine acids (*i.e.*, serine), inducing the inhibition of the catalytic activity of AChE.[1] Moreover, the phosphorylation-induced inactivation of AChE in the body can cause the accumulation of the neurotransmitter acetylcholine *in vivo*, resulting in the disturbance of cholinergic receptor activity to cause serious clinical complications (*i.e.*, respiratory tract and fibrillation) and even death.[3] Therefore, the development of rapid, sensitive, and selective detection methods is urgently desirable for the evaluation of the catalysis and phosphorylation of AChE especially monitoring OPs towards the rapid early warning and accurate diagnosis of OP exposure.

To date, numerous detection strategies have been widely applied for monitoring OP exposure,[4–20] especially the ones for quantifying the direct biomarkers of OP exposure of free OPs based on the specific OP-induced inhibition of catalytic activity of AChE that are recognized to be highly sensitive and selective.[9,11,13,15,16,20] These measurement methods for OP tests mainly

[a]*Shandong Province Key Laboratory of Life-Organic Analysis, School of Chemistry and Chemical Engineering, Qufu Normal University, Qufu City, Shandong Province 273165, P. R. China. E-mail: huawangqfnu@126.com; Fax: +86 537 4456306; Tel: +86 537 4456306*

[b]*School of Mechanical and Materials Engineering, Washington State University, Pullman, WA 99164, USA*

include gas chromatography (GC),[4–6] high performance liquid chromatography (HPLC),[7,8] electrochemical tests,[9–11] colorimetric assays,[12–14] and fluorescent detections.[15–20] Comparing the chromatography evaluations and electrochemical analysis methods that need either time-consuming operation or complicated labelling and modification procedures, fluorimetric methodologies stand out as rapid, sensitive, and efficient especially in combination with the nanotechnologies and fluorescent nanomaterials, mostly known as semiconductor quantum dots (QDs).[15,18,20] Inorganic fluorescent nanomaterials can possess some advantages over traditional organic fluorescent dyes, including high fluorescence intensity, good stability, spectral line width, and sustainable luminous, making them increasingly used as fluorescent nanoprobes for detecting various OP biomarkers in biomedicine, food hygiene, and environmental monitoring.[18–20] Typically, some fluorescence assays have employed QDs for detection of free OPs including the evaluation of AChE activity.[15,18,20] For example, Yu *et al.* have proposed a sensitive sensing system for the analysis of OPs with photoluminescent QDs.[18] Zheng and coworkers described pesticide biosensors using nanostructured AChE films and CdTe QDs.[20] The use of QDs of heavy metal ions, however, may suffer from potential toxicity and complicated synthetic procedures.[19] In particular, the labelling or release of heavy metal ions during the procedure of enzyme-catalysed reactions may cause the denaturation and activity inhibition of cholinesterase (*i.e.*, AChE), in addition to potential environmental endangerment.[19–21] Accordingly, developing more reliable, label-free, and continuous investigation systems alternatively using biocompatible florescent probes to achieve physiologically friendly "green" reaction environments to achieve the improved evaluation of the catalysis and phosphorylation of AChE and AChE-based analysis of OPs is of great interest.

In recent years, there have emerged new kinds of fluorescent nanomaterials of noble metal nanoclusters such as gold nanoclusters (AuNCs) and silver nanoclusters.[22–28] These nanoclusters possess some unique properties, including ultra-small size, non-toxicity, high biocompatibility, and strong fluorescence. However, most of the applications are for the analysis of routine substances such as heavy metal ions, dopamine, and glucose.[22–25,27,28] For example, Zhang *et al.* reported a selective method for the detection of Cu^{2+} using glutathione-protected fluorescent AuNCs.[22] Alternatively, in this work, a sensitive, simple, and rapid fluorimetric method has been proposed by way of "lab-on-a-drop" with biocompatible AuNCs as highly fluorescent nanoprobes for the label-free evaluation of the catalysis and OP-induced inhibition of AChE activity towards the quantitative determination of OPs. The main fluorimetric analysis procedure is illustrated schematically in Scheme 1. Herein, bovine serum albumin (BSA)-stabilized gold nanoclusters (BSA-AuNCs) were prepared and mixed with acetylthiocholine (ATC) to serve as "a drop" of fluorimetric reaction substrate for probing the catalytic activity and phosphorylation of AChE, and further detecting OPs using dimethyl-dichlorovinyl phosphate (DDVP) as an OP model. The release of thiocholine from the AChE-catalyzed hydrolysis of ATC would cause the aggregation of AuNCs so as to decrease their fluorescence intensity, depending on the catalytic activity of AChE. Moreover, the presence of OPs (*i.e.*, DDVP) in the reaction system could conduct the specific inhibition of AChE activity, so that a highly sensitive and selective quantification of OPs could be expected. To the best of our knowledge, this is the first report on the label-free systematic evaluation of catalytic activity and phosphorylation reaction of AChE has been realized under a physiologically friendly environment by way of a "lab-on-a-drop" with biocompatible fluorescent nanoprobes of AuNCs, in combination with sensitive fluorimetric outputs. The application feasibility of the AuNCs-based fluorimetry for quantifying low-level OP residues in vegetable samples has been demonstrated with high detection sensitivity and selectivity.

2. Experimental section

2.1. Chemicals and materials

Tetrachloroauric(III) acid ($HAuCl_4 \cdot 3H_2O$, >99.9%), bovine serum albumin (BSA), acetylthiocholine (ATC), acetylcholinesterase (AChE) were purchased from Sigma-Aldrich (Beijing, China). Dimethyl-dichloro-vinyl phosphate (DDVP) was provided by Dibai Reagents (Shanghai, China). Vitamin C (V_C), vitamin B_1 (V_{B_1}), vitamin B_2 (V_{B_2}), $FeCl_3$, NaCl, $MgCl_2$, $ZnCl_2$, KCl, $CaCl_2$, Na_3PO_4, glucose (Glu), and fructose (Fru) were purchased from Beijing Chemical Reagent Co. (Beijing, China). All chemicals used were of analytical grade, and all glass containers were cleaned by *aqua regia* and ultrapure water.

2.2. Apparatus

The fluorescence measurements were conducted using a fluorescence spectrophotometer (F-7000, Hitachi, Japan) operated at an excitation wavelength at 470 nm with both excitation and emission slit widths of 5.0 nm. The fluorescence intensities were collected at ~634 nm. Transmission electron microscopy (TEM, Tecnai G20, FEI, USA) images were recorded at 100 kV. High-performance liquid chromatography (HPLC) (Agilent 1200, USA) analysis was performed on a Zorbax SB-C18 column (150 mm × 4.6 mm).

2.3. Synthesis of protein-stabilized Au nanoclusters

The protein-stabilized fluorescent Au nanoclusters (AuNCs) were prepared with BSA as the protein stabilization and reduction agents following a modified synthetic route reported previously.[26] Briefly, aqueous $HAuCl_4$ solution (1.0 mL, 10 mM) was added to a BSA solution (1.0 mL, 50 mg mL^{-1}) under vigorous stirring at 37 °C for 10 min. Then, NaOH solution (0.10 mL, 1.0 M) was introduced and vigorously stirred at 37 °C for 12 h. Finally, the resultant solution was dialyzed in water for 48 h, and the BSA-stabilized AuNCs were stored at 4 °C for future use.

2.4. Preparation of stock OP solutions of DDVP

The stock solution of OPs was prepared by using DDVP as an example. An aliquot of DDVP was dissolved in 5.0 mL of hexane and stored in a refrigerator at 4 °C for further use. Different

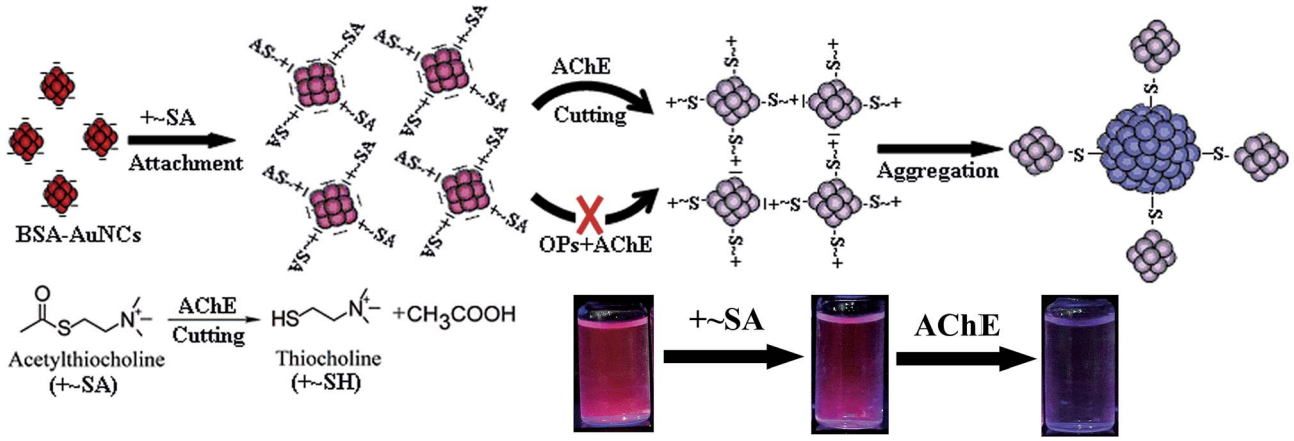

Scheme 1 A schematic illustration of the fluorimetric assay procedure with fluorescent changes of BSA-stabilized AuNCs (BSA-AuNCs), including the AChE-catalyzed hydrolysis of ATC and the phosphorylation-induced inhibition of AChE catalysed activities by OPs.

DDVP concentrations were obtained by freshly diluting the DDVP stock solution with isopropanol.

2.5. Fluorimetric evaluations of AChE catalytic activity

An aliquot of fluorimetric reaction substrate consisting of 225 μL AuNCs (1.25 mM) and 25 μL of ATC (500 μM) was added to six tubes (0.5 mL). Each of the 25 μL AChE solutions with different catalytic activities of 0.0, 0.00005, 0.0005, 0.0050, 0.050, 0.50 U mL^{-1} were then introduced. After that, the resultant mixtures of catalysed reactions were separately incubated at 37 °C for 1 h. Subsequently, the fluorescence spectra of the reaction mixtures were recorded depending on the catalytic activity of AChE. Herein, the quenching efficiencies of AuNCs by thiocholine released from the AChE-catalyzed ATC hydrolysis were calculated according to the equation: quenching efficiency $= (F_0 - F)/F_0$, where F_0 and F refer to the fluorescence intensities of AuNC nanoprobes, which reached the maximum, before and after the AChE-catalytic ATC reactions at different conditions, respectively.

2.6. Fluorimetric analysis of DDVP

An aliquot of the 25 μL DDVP solutions with different concentrations (0.0, 3.2×10^{-5}, 1.6×10^{-4}, 0.8×10^{-3}, 0.4×10^{-2}, and 2.0×10^{-2} μM) was mixed with 25 μL of AChE (0.5 U mL^{-1}) to be incubated for 1 h. An amount of fluorimetric reaction substrate consisting of 225 μL of AuNCs (1.25 mM) and 25 μL of ATC (500 μM) was introduced to each of the above reactant solutions and incubated at 37 °C for 1 h. Furthermore, the fluorescence spectra of the reaction mixtures were recorded at ~634 nm. The DDVP inhibition efficiencies of AChE catalysis were calculated according to the equation: inhibition efficiency $= (F_x - F)/(F_0' - F)$,[16] where F_0' refers to the fluorescence intensities of "a drop" of fluorimetric reaction substrate consisting of AuNCs with ATC; and F and F_x refer to the fluorescence intensities of AuNC nanoprobes with AChE-catalytic ATC reaction substrates in the absence and presence of DDVP, respectively.

Moreover, the detection selectivity of the developed fluorometric assay for DDVP was examined accordingly for potential interferents of 0.020 μM vitamin C (V_C), vitamin B_1 (V_{B_1}), vitamin B_2 (V_{B_2}), Fe^{3+}, Na^+, Mg^{2+}, Zn^{2+}, K^+, Ca^{2+}, PO_4^{3-}, glucose (Glu), and fructose (Fru) and compared with 0.0040 μM of DDVP.

2.7. Preparation and analysis of vegetable samples of DDVP residues

Vegetable samples of Chinese cabbage were pre-treated on site in a vegetable field with DDVP, and then experimentally processed according to a modified procedure.[29] Briefly, 20 g of DDVP-treated samples of Chinese cabbage were finely chopped, and then dissolved in 100 mL methanol to be ultra-sonicated for 60 min. After that, the sample mixtures were centrifuged to obtain the supernatants and further filtered, and then the impurities such as pigments in the filtrates were removed with activated carbon. Subsequently, the DDVP residue-containing samples were washed with 20 mL of methanol, and then dried at 50 °C using a vacuum rotary evaporator. The concentrations of the DDVP residues in the samples were measured using high-performance liquid chromatography (HPLC) (Agilent 1200, USA) with a Zorbax SB-C18 column at 25 °C. Moreover, a certain amount of DDVP sample with the measured concentration was diluted into different concentrations of DDVP residues for the fluorimetric assays, according to the same analysis procedure above. In addition, the detections of some DDVP-containing vegetable samples were comparably conducted using the HPLC and the fluorimetric assay.

3. Results and discussion

3.1. The detection mechanism and procedure of the "lab-on-a-drop"-based fluorimetric method

The fluorimetric assay procedure using fluorescent nanoprobes of AuNCs is illustrated schematically in Scheme 1, including the AChE-catalyzed hydrolysis of ATC and the OP-induced inhibition of AChE catalytic activity. Here, BSA-stabilized AuNCs (BSA-AuNCs) that were synthesized at about pH 12 were negatively charged, since the isoelectric point of BSA capped on AuNCs is

at pH 4.7.[30] Once the positively charged ATC was introduced, it can be adsorbed onto the surfaces of the oppositely charged AuNCs *via* electrostatic interactions to form "a drop" of fluorimetric reaction substrate. Furthermore, AChE was added into the above reaction substrate to catalyze the hydrolysis of ATC to produce thiocholine with positively charged and additional thiol (–SH) groups. The obtained thiocholine could then cap onto the BSA-AuNCs surface through electrostatic interactions, hydrogen bonds, and metal–thiol bonding. An aggregation procedure of the AuNCs would cause a great decrease in the fluorescence intensity, which depends on the catalytic activity of AChE. Alternatively, when the OPs were applied into the reaction system, they inhibit the catalytic activity of AChE as aforementioned. As a result, the thiocholine released from the AChE-catalyzed hydrolysis of ATC could decrease; thus, the aggregation and decrease in the fluorescence of BSA-AuNCs might be curbed to some degree. Therefore, the proposed fluorimetric system, by way of "lab-on-a-drop" with biocompatible fluorescent nanoprobes of AuNCs, should be tailored for the evaluation of AChE activity under physiologically simulated environment towards the analysis of OPs with high sensitivity and selectivity, as will be demonstrated later.

3.2. Characterization of the AuNCs-based fluorimetric measurement procedure

In order to clarify the "lab-on-a-drop"-based fluorimetric procedure above, characterization of the morphological features of AuNCs was conducted by transmission electron microscopy (TEM) before and after the addition of ATC, followed by the AChE-catalyzed hydrolysis to release thiocholine (Fig. 1). It can be seen that the average size of AuNCs is about 0.8 nm (Fig. 1A). The addition of ATC to AuNCs might have little effect on the size of AuNCs (Fig. 1B), of which the AuNCs-ATC would serve as "a drop" of fluorimetric reaction substrate. Furthermore, one can note that the introduction of AChE could induce the large aggregation of AuNCs (Fig. 1C). Accordingly, the TEM images supported the description and interpretation

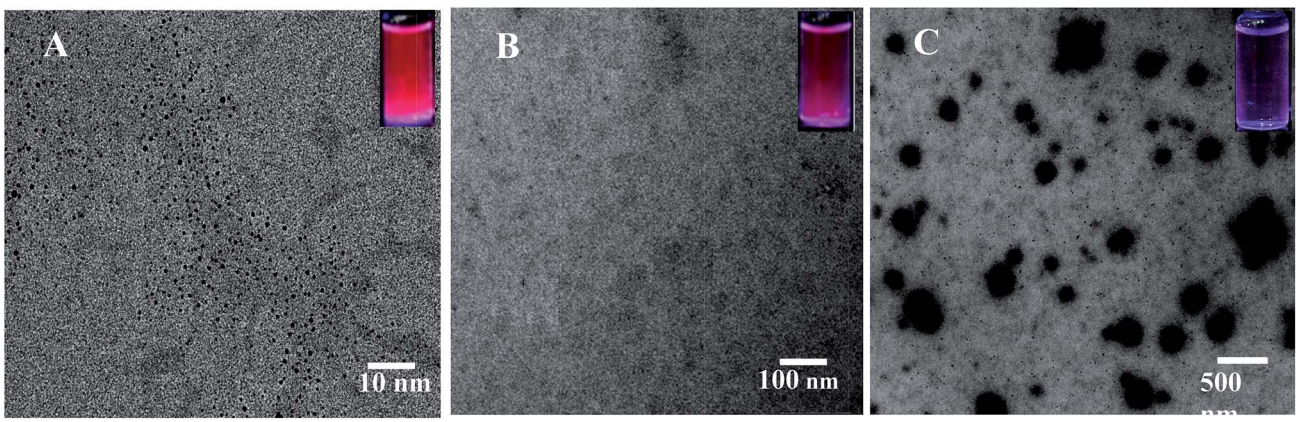

Fig. 1 TEM images of (A) AuNCs alone, and in the presence of (B) ATC, and (C) ATC with AChE. (Inset: photographs under UV light at 365 nm).

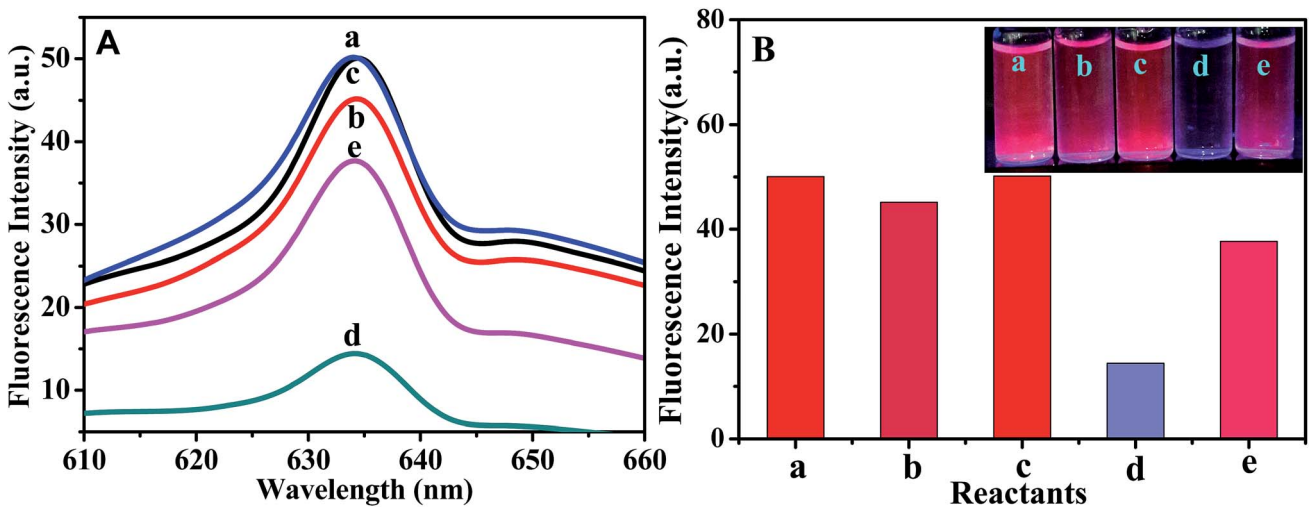

Fig. 2 (A) Fluorescence spectra and (B) corresponding fluorescence intensities of the reactants of (a) 1.25 mM AuNCs alone, and in the presence of (b) 50 μM ATC, (c) 0.05 U mL^{-1} of AChE, (d) 50 μM ATC with 0.05 U mL^{-1} of AChE, and (e) 50 μM ATC with 0.05 U mL^{-1} of AChE and 0.004 μM DDVP, of which the reactants were added to AuNCs in a step-by-step way (inset: photographs under UV light).

of AuNCs in the detection mechanism and procedure above. Moreover, the procedures were also monitored by fluorimetric measurements, where the fluorescence changes of reactants added step-by-step were recorded including fluorescence spectra, intensities and photographs (Fig. 2). As shown in Fig. 2A, the AuNCs displayed a strong fluorescence at ~634 nm, corresponding to the fluorescence intensity in Fig. 2B(a) and the photographs (insets). It was observed that when ATC was mixed with AuNCs, the fluorescence intensity would slightly decrease due to electrostatic interactions aforementioned (Fig. 2A(b) and B(b)). Furthermore, the introduction of AChE could start the AChE-catalyzed hydrolysis of ATC to produce thiocholine. A significantly quenched fluorescence was observed, as clearly manifested in Fig. 2A(d) and B(d). However, AChE showed no significant influence on the fluorescence of the AuNCs (Fig. 2A(c) and B(c)). This demonstrates that the above fluorescence changes result from the AChE-catalyzed hydrolysis of ATC. However, when AChE was pre-exposed to a certain amount of DDVP, the decrease in the fluorescence of the AuNCs was largely suppressed to some degree (Fig. 2A(e) and B(e)) due to the phosphorylation-induced inhibition of AChE catalytic activity. Note that all fluorescence changes are consistent with the photographs recorded under UV light (Fig. 2B (inset)). Consequently, the "lab-on-a-drop"-based fluorimetric analysis procedure could be established for the evaluation of AChE catalytic activity, as well as the detection of Ops, using biocompatible AuNCs as fluorescent nanoprobes.

3.3. Optimization of the reaction conditions of fluorimetric assays

The key detection conditions for the developed fluorimetric assays were optimized, including the amount of AuNCs, ATC

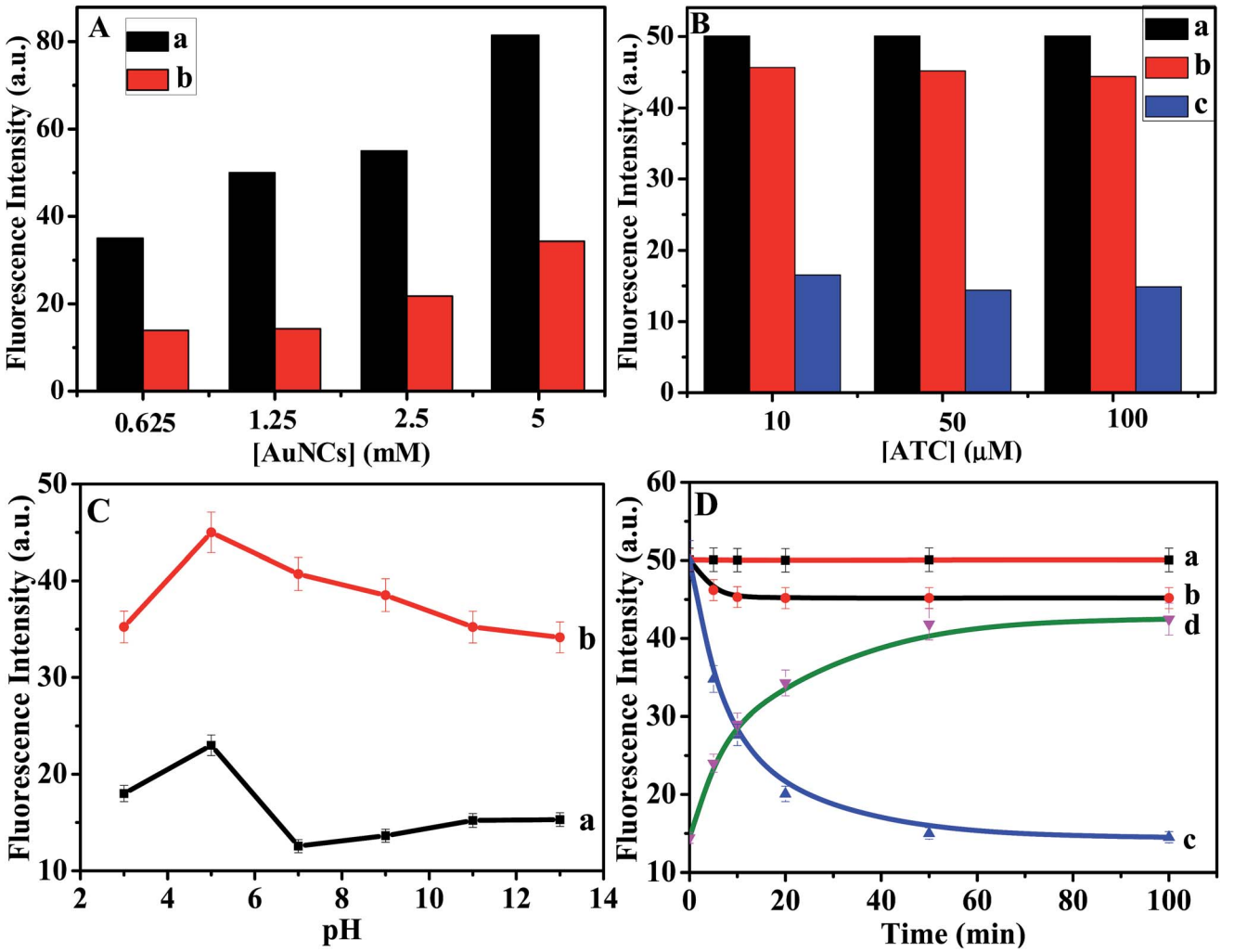

Fig. 3 (A) AuNCs concentration-dependent fluorescence intensities for (a) only AuNCs at different concentrations, and (b) in the presence of 50 μM ATC and 0.05 U mL^{-1} of AChE; (B) ATC concentration-dependent fluorescence intensities for (a) only 1.25 mM AuNCs, and in the presence of (b) ATC at different concentrations, and (c) ATC at different concentrations with 0.05 U mL^{-1} of AChE; (C) the pH-dependent fluorescence intensities for 1.25 mM AuNCs in the presence of (a) 50 μM ATC with 0.05 U mL^{-1} of AChE, and (b) 50 μM ATC, 0.05 U mL^{-1} of AChE, and 0.004 μM of DDVP, of which the samples were incubated for 1 h at different pH values; (D) reaction time-dependent fluorescence intensities for (a) only AuNCs, and in the presence of (b) 50 μM ATC, (c) 50 μM ATC and 0.05 U mL^{-1} of AChE, and (d) 0.004 μM of DDVP and AChE (0.05 U mL^{-1}), of which the reaction solution was taken out at the defined time intervals to be mixed with 50 μM of ATC for fluorescence monitoring.

concentrations, reaction time, and pH values (Fig. 3). Herein, the quenching efficiencies of the AuNCs by thiocholine released from the AChE-catalyzed ATC hydrolysis were calculated according to the equation for quenching efficiencies defined with the details shown in the Experimental section.

3.3.1. AuNCs amount for catalysis reactions. Since the sensitivity of the detection method is reflected by the variation of fluorescence intensity, the amount of AuNCs is an important factor. Fig. 3A shows the dependence of fluorescence intensity on the amounts of AuNCs with different concentrations, which were calculated from the $HAuCl_4$ concentration. With increase in the concentration of AuNCs, the fluorescence increased gradually (Fig. 3A(a)). However, when ATC and AChE were applied in order, their fluorescence intensities decreased with different quenching efficiencies (Fig. 3A(b)). Obviously, the highest quenching efficiency was obtained at a concentration of AuNCs at 1.25 mM, which was selected thereafter.

3.3.2. ATC concentration for catalysis reactions. Fig. 3B shows the effects of ATC concentration on the fluorescence intensities of AuNCs before (Fig. 3B(b)) and after (Fig. 3B(c)) the addition of AChE, where the original AuNCs were used as the control (Fig. 3B(a)). One can note that the highest quenching efficiency for the AChE-catalysis reaction solution could be achieved at 50 μM of ATC, serving as the optimum one to be chosen. Higher ATC concentration (*i.e.*, 100 μM) showed no significant change in fluorescence intensity. However, too high ATC concentration might have the risk of a large accumulation of positively charged ATC, resulting in the aggregation of AuNCs nanoprobes prior to the AChE catalysed reactions, as observed elsewhere for silver nanoparticles.[31]

3.3.3. The pH values of the catalytic and phosphorylation reactions. The pH value is another important factor governing the fluorimetric detection system. Fig. 3C exhibits the pH-dependent fluorescence intensities of the reaction solutions, of which the AChE catalysed and DDVP phosphorylation reactions were conducted at different pH values. It was found that the highest fluorescence intensity might be obtained with precipitation at pH ~ 5.0, presumably because of the charge neutrality of the BSA-stabilized AuNCs (the isoelectric point of BSA at pH 4.7). However, the suitable pH range for the AChE catalysed and DDVP phosphorylation reactions were found to be from pH 7.0 to 9.0, as determined by the largest fluorescence quenching and inhibition efficiencies.

3.3.4. Reaction time of catalysis and phosphorylation reactions. Fig. 3D shows the plots of fluorescence intensities *versus* the reaction time for the AChE catalysed and DDVP-induced phosphorylation reactions with AuNCs and the fluorimetric reaction substrate of AuNCs and ATC as the controls. One can find that the two controls showed no significant changes in the fluorescence intensities of the AuNCs over time (Fig. 3D(a) and (b)). However, as time went by, the addition of AChE makes the fluorescence intensities decrease gradually to reach a plateau after 1 h (Fig. 3D(c)). Moreover, the reaction time for DDVP-inhibited AChE catalysis was also optimized as 1 h, during which the quenching of the fluorescence of the AuNCs was mainly suppressed by the DDVP phosphorylation of AChE (Fig. 3D(d)), showing an increasing fluorescent intensity.

3.4. Evaluation performances of the "lab-on-a-drop"-based fluorimetric assay system

Under the optimum experimental conditions, the capabilities of the fluorimetric assay system for the label-free evaluation of AChE catalytic activity was investigated. Fig. 4A displays the fluorescence spectra of the fluorimetric AuNCs-ATC reaction substrate and various use of AChE. As shown in Fig. 4A, the fluorescence intensities of AuNCs decreased gradually with an increasing concentration of AChE in catalytic activity units. The relationship between the AChE activity units and fluorescence quenching efficiencies, which were calculated according to the equation detailed in the Experimental section, was described in

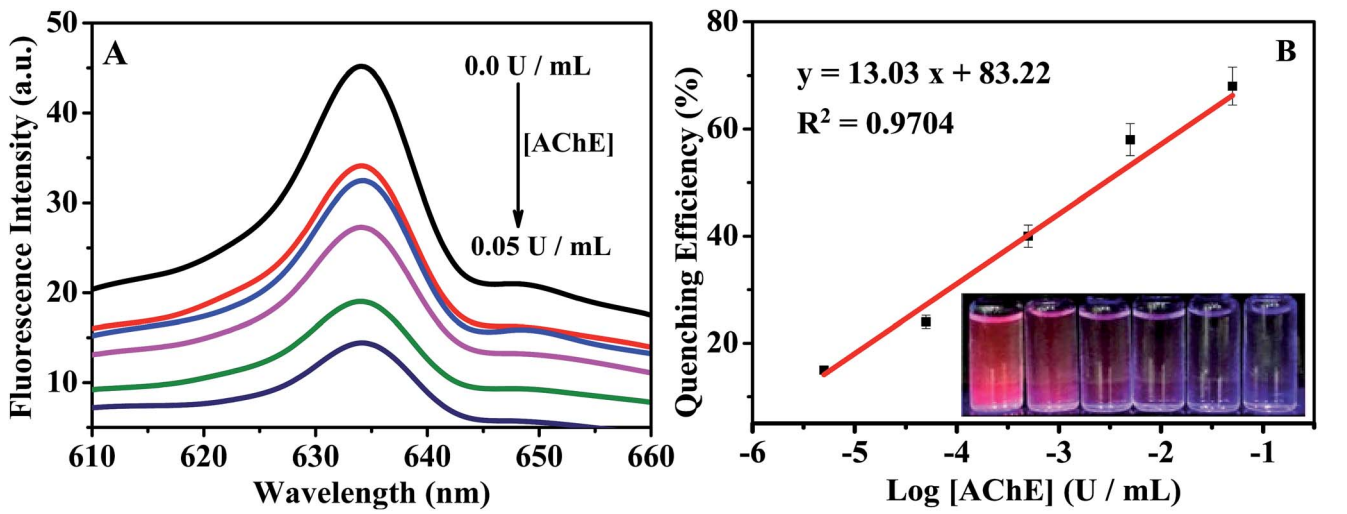

Fig. 4 (A) Fluorescence spectra of the fluorimetric reaction substrate (1.25 mM AuNCs and 50 μM ATC) in the presence of different AChE concentrations of 0.0, 0.000005, 0.00005, 0.0005, 0.005, and 0.05 U mL^{-1}; (B) fluorescence quenching efficiencies *versus* the logarithmic activity units of AChE (inset: photographs under UV light at 365 nm).

Fig. 4B, corresponding to photographs under UV light (Fig. 4B (inset)).

A linear range of AChE concentrations was obtained ranging from 5.0×10^{-6} to 5.0×10^{-2} U mL^{-1} ($R^2 = 0.9704$) with the detection limit down to 2.0×10^{-6} U mL^{-1}. Accordingly, with biocompatible fluorescent nanoprobes of AuNCs, the present fluorimetric method can allow for the evaluation of AChE catalytic activity under physiologically friendly environments so as to facilitate the catalytic inhibition-based detection of OPs with high sensitivity and selectivity, as demonstrated afterwards.

The quantitative detection abilities of the fluorimetric assay for DDVP as an OP model were investigated on the basis of the phosphorylation-induced inhibition of AChE catalytic activity (Fig. 5). As shown in Fig. 5A, the fluorescence intensities of AuNCs increased with an increasing concentrations of DDVP, as also evidenced by the photographs under UV light (Fig. 5B (insert)). The calibration curve was obtained with the DDVP

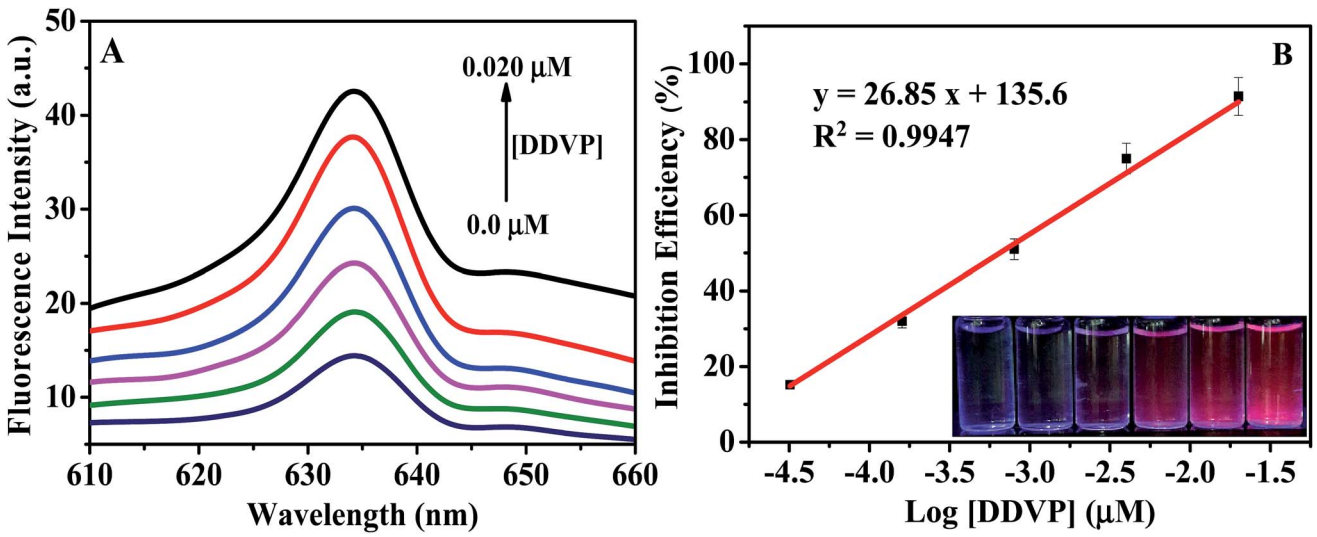

Fig. 5 (A) Fluorescence spectra of the catalysed reaction solution (1.25 mM AuNCs, 50 μM ATC, 0.050 U mL^{-1} of AChE) mixed with DDVP at different concentrations of 0.0, 3.2×10^{-5}, 1.6×10^{-4}, 0.8×10^{-3}, 0.4×10^{-2}, and 2.0×10^{-2} μM; (B) the fluorescent inhibition efficiencies of DDVP *versus* the logarithmic concentrations of DDVP (inset: photographs under UV light at 365 nm).

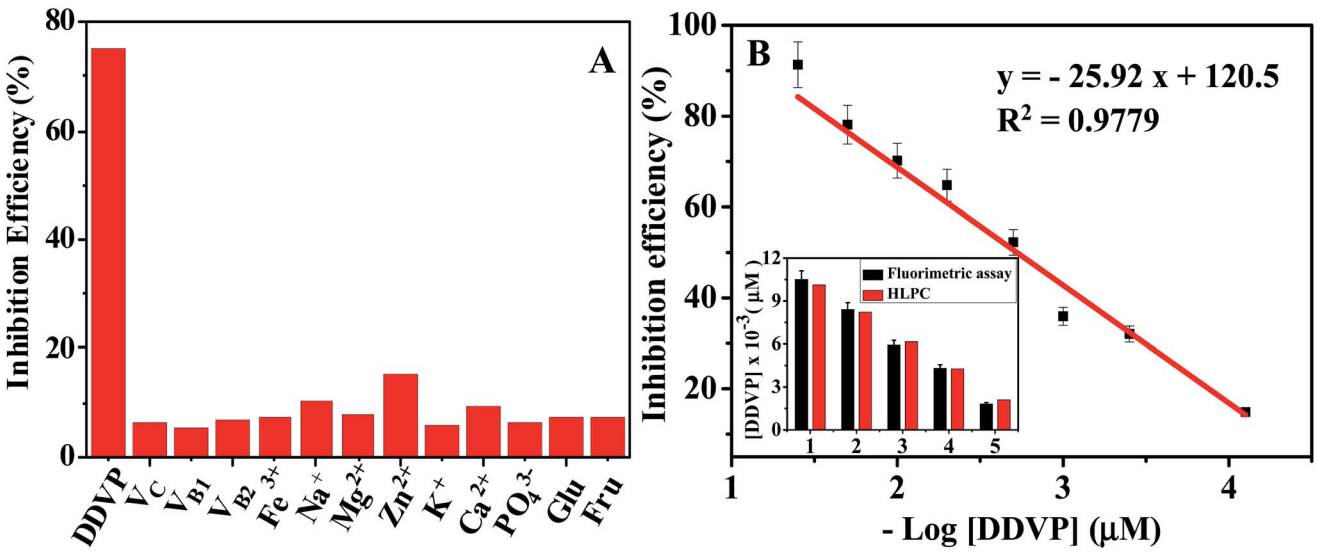

Fig. 6 (A) Comparison of fluorescent inhibition efficiencies among the potential interferents of 0.020 μM of vitamin C (V_C), vitamin B_1 (V_{B_1}), vitamin B_2 (V_{B_2}), Fe^{3+}, Na^+, Mg^{2+}, Zn^{2+}, K^+, Ca^{2+}, PO_4^{3-}, glucose (Glu), and fructose (Fru), comparing to 0.0040 μM DDVP, which were added into the fluorescence catalysis reaction solution (1.25 mM AuNCs, 50 μM ATC, and 0.05 U mL^{-1} of AChE) to be measured under optimized conditions; (B) calibration curve for the analysis of DDVP residues in vegetable samples of different concentrations (0.0, 8.0×10^{-5}, 4.1×10^{-4}, 0.12×10^{-2}, 0.23×10^{-2}, 0.51×10^{-2}, 1.2×10^{-2}, 2.2×10^{-2}, and 4.1×10^{-2} μM) by plotting the inhibition efficiencies *versus* the-logarithmic concentrations of DDVP, and the relation of analysis results between the HPLC and the fluorimetric assay for the detection of DDVP residues in vegetable samples (1 to 5) (inset).

concentrations linearly ranging from 3.2×10^{-5} to 2.0×10^{-2} μM ($R^2 = 0.9947$) with the detection limit down to 13.67 pM (defined as the concentration of inhibitor required to achieve 5% inhibition),[32] showing a considerably high detection sensitivity.

Moreover, the detection selectivity of the developed fluorimetric assay for DDVP was examined by using some potential interfering substance, including vitamin C (V_C), vitamin B_1 (V_{B_1}), vitamin B_2 (V_{B_2}), Fe^{3+}, Na^+, Mg^{2+}, Zn^{2+}, K^+, Ca^{2+}, PO_4^{3-}, glucose (Glu), and fructose (Fru) (Fig. 6A). It is observed that compared to DDVP, these common ions and organic compounds presented negligibly low inhibition efficiencies to the catalytic activity of AChE, indicating that they showed no interference for the determination of DDVP under the optimized assay conditions. In addition, other kinds of OPs including the commonly used methidathion and paraoxon have also been tested, showing the inhibition efficiencies comparable to that of DDVP (data not shown). Accordingly, the developed AuNCs-based fluorimetric approach can determine the total free OPs with high selectivity and anti-interference abilities.

3.5. Preliminary detection applications for DDVP residues in vegetable samples

To evaluate the feasibility of their practical applications, the present fluorimetric assay was utilized for the detection of DDVP residues in samples of Chinese cabbage. Herein, the concentrations of DDVP residues in samples were first determined using high-performance liquid chromatography (HPLC), and then diluted into different DDVP concentrations for the fluorimetric assays. The calibration curve for DDVP residues in the samples was thus obtained with the results shown in Fig. 6B. One can find that the logarithmic concentrations of DDVP residues linearly depends on the inhibition efficiencies (defined in the Experimental section) in the range of 8.0×10^{-5} to 4.1×10^{-2} μM DDVP with the detection limit down to ~36 pM. Note that the detection limit is much lower than the maximum residue limits reported in the European Union pesticides database of 0.010 mg kg^{-1} (~64 pM) for DDVP (http://ec.europa.eu/sanco_pesticides). Moreover, a comparison of detection abilities between the classic HPLC and the developed fluorimetric assay was carried out for some DDVP residue-containing vegetable samples (Fig. 6B (Inset)), both showing a high relation in the analysis results. Therefore, the developed "lab-on-a-drop"-based fluorimetric method has potential as a reliable and sensitive strategy for the detection of pesticide residues (*i.e.*, DDVP) in real samples of vegetables.

4. Conclusions

In the present work, protein-stabilized AuNCs have been applied initially as biocompatible fluorescent nanoprobes for the label-free evaluation of the catalytic hydrolysis and phosphorylation of AChE under physiologically simulated environments. "A drop" of fluorimetric reaction substrate consisting of AuNCs and a ATC mixture was employed to facilitate the rapid "lab-on-a-drop" fluorimetric measurements (fluorescence quenching and inhibition efficiencies) to monitor the procedures of catalysed and phosphorylation-induced inhibition reactions of AChE, which were also characterized by high-resolution electronic microscopy imaging. Moreover, a simple, rapid and highly sensitive and selective fluorimetric analysis method has thereby been successfully established for probing the exposure to total free OPs of pesticide residues in vegetables by using dimethyl-dichloro-vinyl phosphate (DDVP) as an example. Investigation results demonstrate that the developed AuNCs-based fluorimetric method can possess some outstanding advantages over the traditional detection methodologies in monitoring the AChE catalytic activity and the detection of free OPs. First, the use of biocompatible fluorescent nanoprobes of AuNC could allow for the evaluation of AChE catalytic activity under physiologically simulated environments, thus avoiding the possible denaturation and toxic inactivity of AChE. Second, the combination of efficient hydrolytic catalysis and specific phosphorylation inhibition of AChE activity with sensitive fluorimetric outputs could enable the detection of OPs with high selectivity and sensitivity (down to ~36 pM DDVP in vegetables). Third, simple and label-free analysis procedures ("a drop") could facilitate the rapid detection of total free OPs. Therefore, such a "lab-on-a drop"-based detection strategy may pave the way towards the wide applications for the evaluation of physiologic catalytic activity of various enzymes (*i.e.*, cholinesterase) and especially for monitoring the direct phosphorylation biomarkers of free OPs towards rapid early warning and accurate diagnosis of the exposure to OPs in the environment (*i.e.* pesticides), battlefields (*i.e.*, nerve agents), and clinical laboratories.

Acknowledgements

This work is supported by the National Natural Science Foundations of China (no. 21375075, 21302109, and 21302110), the Taishan Scholar Foundation of Shandong Province, and the Natural Science Foundation of Shandong Province (ZR2013BQ017 and ZR2013BM007), P. R. China.

Notes and references

1 H. Li, J. Guo, H. Ping, L. Liu, M. Zhang, F. Guan, C. Sun and Q. Zhang, *Talanta*, 2011, **87**, 93–99.
2 F. Yang, J. R. Wild and A. J. Russell, *Biotechnol. Prog.*, 1995, **11**, 471–474.
3 W. J. Donarski, D. P. Dumas, D. P. Heitmeyer, V. E. Lewis and F. M. Raushel, *Biochemistry*, 1989, **28**, 4650–4655.
4 A. Fidder, A. Hulst, D. Noort, R. De Ruiter, M. Van der Schans, H. Benschop and J. P. Langenberg, *Chem. Res. Toxicol.*, 2002, **15**, 582–590.
5 L.-J. Qu, H. Zhang, J.-H. Zhu, G.-S. Yang and H. Y. Aboul-Enein, *Food Chem.*, 2010, **122**, 327–332.
6 M. K. Chai and G. H. Tan, *Food Chem.*, 2009, **117**, 561–567.
7 T. Pérez-Ruiz, C. Martínez-Lozano, V. Tomás and J. Martín, *Anal. Chim. Acta*, 2005, **540**, 383–391.

8 C. Padrón Sanz, R. Halko, Z. Sosa Ferrera and J. Santana Rodríguez, *Anal. Chim. Acta*, 2004, **524**, 265–270.
9 Y. Li, Z. Gan, Y. Li, Q. Liu, J. Bao, Z. Dai and M. Han, *Sci. China: Chem.*, 2010, **53**, 820–825.
10 Y. Zhang, H. Wang, J. Nie, Y. Zhang, G. Shen and R. Yu, *Biosens. Bioelectron.*, 2009, **25**, 34–40.
11 H. Wang, J. Wang, C. Timchalk and Y. Lin, *Anal. Chem.*, 2008, **80**, 8477–8484.
12 J. Gabaldon, A. Maquieira and R. Puchades, *Talanta*, 2007, **71**, 1001–1010.
13 M. Wang, X. Gu, G. Zhang, D. Zhang and D. Zhu, *Langmuir*, 2009, **25**, 2504–2507.
14 D. Liu, W. Chen, J. Wei, X. Li, Z. Wang and X. Jiang, *Anal. Chem.*, 2012, **84**, 4185–4191.
15 Z. Chen, X. Ren and F. Tang, *Chin. Sci. Bull.*, 2013, **58**, 2622–2627.
16 M. Wang, X. Gu, G. Zhang, D. Zhang and D. Zhu, *Anal. Chem.*, 2009, **81**, 4444–4449.
17 S.-W. Zhang and T. M. Swager, *J. Am. Chem. Soc.*, 2003, **125**, 3420–3421.
18 T. Yu, T.-Y. Ying, Y.-Y. Song, Y.-J. Li, F.-H. Wu, X.-Q. Dong and J.-S. Shen, *RSC Adv.*, 2014, **4**, 8321.
19 R. Hardman, *Environ. Health Perspect.*, 2006, 165–172.
20 Z. Zheng, Y. Zhou, X. Li, S. Liu and Z. Tang, *Biosens. Bioelectron.*, 2011, **26**, 3081–3085.
21 D. Du, W. Chen, W. Zhang, D. Liu, H. Li and Y. Lin, *Biosens. Bioelectron.*, 2010, **25**, 1370–1375.
22 G. Zhang, Y. Li, J. Xu, C. Zhang, S. Shuang, C. Dong and M. M. Choi, *Sens. Actuators B*, 2013, **183**, 583–588.
23 J. Xie, Y. Zheng and J. Y. Ying, *Chem. Commun.*, 2010, **46**, 961–963.
24 Y. Tao, Y. Lin, J. Ren and X. Qu, *Biosens. Bioelectron.*, 2013, **42**, 41–46.
25 X. Xia, Y. Long and J. Wang, *Anal. Chim. Acta*, 2013, **772**, 81–86.
26 J. Xie, Y. Zheng and J. Y. Ying, *J. Am. Chem. Soc.*, 2009, **131**, 888–889.
27 C. Guo and J. Irudayaraj, *Anal. Chem.*, 2011, **83**, 2883–2889.
28 H. Liu, X. Zhang, X. Wu, L. Jiang, C. Burda and J.-J. Zhu, *Chem. Commun.*, 2011, **47**, 4237–4239.
29 T. Pérez-Ruiz, C. Martínez-Lozano, V. Tomás and J. Martín, *Talanta*, 2001, **54**, 989–995.
30 Z. Lin, F. Luo, T. Dong, L. Zheng, Y. Wang, Y. Chi and G. Chen, *Analyst*, 2012, **137**, 2394–2399.
31 Z. Li, Y. Wang, Y. Ni and S. Kokot, *Sens. Actuators B*, 2014, **193**, 205–211.
32 J. Abad, F. Pariente, L. Hernandez, H. Abruna and E. Lorenzo, *Anal. Chem.*, 1998, **70**, 2848–2855.